Imaging of Gynecologic Tumors: Comparison of ^{11}C-Choline PET with ^{18}F-FDG PET

Tatsuo Torizuka, MD, PhD[1]; Toshihiko Kanno, BA[1]; Masami Futatsubashi, BA[2]; Hiroyuki Okada, BA[2]; Etsuji Yoshikawa, BA[2]; Fumitoshi Nakamura, BA[1]; Munetaka Takekuma, MD[3]; Makoto Maeda, MD[3]; and Yasuomi Ouchi, MD, PhD[1]

[1]Positron Medical Center, Hamamatsu Medical Center, Hamakita, Japan; [2]Central Research Laboratory, Hamamatsu Photonics K.K., Hamakita, Japan; and [3]Department of Gynecology, Hamamatsu Medical Center, Hamamatsu, Japan

This study was designed to compare the value of PET using ^{11}C-choline with that of PET using ^{18}F-FDG for the diagnosis of gynecologic tumors. **Methods:** We examined 21 patients, including 18 patients with untreated primary tumors and 3 patients with suspected recurrence of ovarian cancer. ^{11}C-choline PET and ^{18}F-FDG PET were performed within 2 wk of each other on each patient. The patients fasted for at least 5 h before the PET examinations, and PET was performed 5 min (^{11}C-choline) and 60 min (^{18}F-FDG) after injection of each tracer. PET images were corrected for the transmission data, and the reconstructed images were visually analyzed. Then, the standardized uptake value (SUV) was calculated for quantitative assessment of tumor uptake. PET results were compared with surgical histology or >6 mo of clinical observations. **Results:** Of 18 untreated patients, ^{11}C-choline PET correctly detected primary tumors in 16 patients, whereas ^{18}F-FDG PET detected them in 14 patients. In 1 patient with small uterine cervical cancer and 1 diabetic patient with uterine corpus cancer, only ^{11}C-choline PET was true-positive. Both tracers were false-negative for atypical hyperplasia of the endometrium in 1 patient and were false-positive for pelvic inflammatory disease in 1 patient. For the diagnosis of recurrent ovarian cancer ($n = 3$), ^{11}C-choline PET and ^{18}F-FDG PET were true-positive in 1 patient, whereas neither tracer could detect cystic recurrent tumor and microscopic peritoneal disease in the other 2 patients. In the 15 patients with true-positive results for both tracers, tumor SUVs were significantly higher for ^{18}F-FDG than for ^{11}C-choline (9.14 $\pm$ 3.78 vs. 4.61 $\pm$ 1.61, $P < 0.0001$). In 2 patients with uterine cervical cancer, parailiac lymph node metastases were clearly visible on ^{18}F-FDG PET but were obscured by physiologic bowel uptake on ^{11}C-choline PET. **Conclusion:** The use of ^{11}C-choline PET is feasible for imaging of gynecologic tumors. Unlike ^{18}F-FDG PET, interpretation of the primary tumor on ^{11}C-choline PET is not hampered by urinary radioactivity; however, variable background activity in the intestine may interfere with the interpretation.

Key Words: ^{11}C-choline PET; ^{18}F-FDG PET; gynecologic tumors; diagnosis

J Nucl Med 2003; 44:1051–1056

Received Oct. 31, 2002; revision accepted Feb. 13, 2003.

For correspondence or reprints contact: Tatsuo Torizuka, MD, PhD, Positron Medical Center, Hamamatsu Medical Center, 5000, Hirakuchi, Hamakita, Shizuoka, 434-0041, Japan.

E-mail: tatsuo@pmc.hmedc.or.jp

Use of PET for detection and localization of cancer in the body is based on its unique capability to evaluate metabolic activity in human neoplasms. The glucose analog ^{18}F-FDG has proven useful as an oncologic PET probe for many forms of cancer on the basis of accelerated rates of glycolysis in malignancies (*1–4*). However, the utility of ^{18}F-FDG PET for detecting malignant tumors in the pelvis is unsatisfying because the abundant radioactivity excreted into the bladder hampers the interpretation of images even after voiding (*5,6*). Bladder irrigation, adequate hydration, or iterative reconstruction of images may minimize but not completely avoid this problem.

Carcinogenesis is characterized by enhanced cell proliferation. Unlike glucose, choline is incorporated in cells through phosphoryl choline synthesis and is integrated in membrane phospholipids (*7*). Malignant transformation of cells is associated with induction of choline kinase activity, resulting in increased levels of phosphoryl choline for the synthesis of membrane phospholipids (*8*). ^{31}P magnetic resonance spectroscopy has revealed an elevated level of phosphoryl choline in various cancers, whereas the choline metabolite is present at a low or undetectable level in normal tissues (*9,10*). These findings may provide the rationale for the use of choline as a tumor-seeking agent.

PET with ^{11}C-choline was first introduced for evaluation of brain tumors (*11,12*). Brain tumors are characterized by enhanced cell membrane synthesis, whereas uptake of ^{11}C-choline by normal brains is low, thus enabling tumor detection by PET. ^{11}C-Choline PET has been more recently studied for imaging prostate cancer (*13,14*). Because ^{11}C-choline shows only minimal radioactivity in the urinary tracts and bladder of fasting individuals, prostate tumor can be visualized more clearly on ^{11}C-choline PET than on ^{18}F-FDG PET. This fact implies that ^{11}C-choline may be feasible for the detection of pelvic tumors; however, little has been known about the interpretation of gynecologic tumors by ^{11}C-choline PET. The present PET study was designed to compare the value of ^{11}C-choline PET with that of ^{18}F-FDG PET for the imaging of gynecologic tumors.

MATERIALS AND METHODS

Patient Population

^{11}C-Choline PET and ^{18}F-FDG PET examinations were performed on 21 patients (age range, 36–77 y; mean age, 60 ± 13 y) with gynecologic tumors (Table 1). Of the 21 patients, 18 patients (patients 1–18) were untreated and underwent PET examinations before surgery to evaluate the primary tumor and nodal staging. Clinical staging was based on the International Federation of Gynecology and Obstetrics (FIGO) system (*15*). Within 1 mo after PET, 15 patients underwent surgery and 3 patients with uterine cervical cancer in stage IIB (parametrial involvement) (patients 13–15) received a transarterial infusion of chemotherapy before surgery. The other 3 patients (patients 19–21) were suspected of having recurrence of ovarian cancer after initial surgery and chemotherapy. The interval between ^{11}C-choline PET and ^{18}F-FDG PET scans ranged from 1 to 15 d (mean, 3.8 d). All patients fasted for at least 5 h before the PET studies because hyperglycemia may reduce tumor ^{18}F-FDG uptake (*16*) and physiologic ^{11}C-choline uptake in the pancreas and small intestine may be enhanced after a meal (*11*). Serum glucose levels measured at the time of ^{18}F-FDG injection were normal in all patients, except for 1 patient with diabetes (patient 10). All patients provided written informed consent for participation in the study, which was approved by the Ethics Committee of Hamamatsu Medical Center.

PET Imaging

The whole-body PET scanner we used was SHR22000 (Hamamatsu Photonics, K.K.) (*17*). The SHR22000 scanner permits simultaneous acquisition of 63 transverse planes of 3.6-mm thickness encompassing a 23.0-cm axial field of view. ^{18}F-FDG was produced according to the standard procedure (*18*). To measure the attenuation factor, transmission scanning was performed with 5 bed positions covering the upper femur to the head for 5 min each on all patients. Static emission scanning was performed over the same area for 6 min per bed position, starting 60 min after intravenous administration of ^{18}F-FDG (400–500 MBq). To reduce the accumulation of ^{18}F-FDG activity in the urinary bladder, patients were asked to void just before the emission scan started.

^{11}C-Choline was synthesized by the reaction of ^{11}C-methyl iodine with dimethylaminoethanol, according to Hara et al. (*11*). For the first 3 patients of this study, we performed dynamic ^{11}C-choline PET imaging to estimate the time course of tumor activity in the pelvis. After 10 min of transmission scanning, dynamic emission scanning was performed after intravenous administration of ^{11}C-choline (500–600 MBq). The dynamic sequence consisted of ten 1-min scans and five 2-min scans for a total scan time of 20 min. The time–activity curve showed that tumor uptake rapidly reached a maximum at 3 min after injection and remained almost constant afterward (Fig. 1). Thus, we decided to start static emission scanning at 5 min after injection of ^{11}C-

TABLE 1
Summary of Patients and Histology of Primary Tumors

Patient no.	Age (y)	Histology of primary tumor	Tumor		Tumor SUV	
			Stage	Size (cm)	^{18}F-FDG	^{11}C-CHO
		Untreated primary tumor (n = 18)				
		Uterine corpus cancer				
1	49	Endometrial adenocarcinoma	IIIA	4	16.81	5.77
2	66	Endometrial adenocarcinoma	IB	1	3.79	2.83
3	72	Endometrial adenocarcinoma	IB	2.5	12.55	5.52
4	42	Endometrial adenocarcinoma	IB	2.5	9.09	6.33
5	62	Endometrial adenocarcinoma	IB	2.2	6.13	4.93
6	40	Endometrial adenocarcinoma	IA	2.5	6.83	3.06
7	63	Endometrial adenocarcinoma	IA	2	6.54	6.79
8	77	Carcinosarcoma	IIIA	4	7.43	3.45
9	72	Carcinosarcoma	IC	3	7.29	2.13
10	74	Clear cell carcinoma	IB	1.7	FN	4.81
11	68	Atypical hyperplasia	0	NA	FN	FN
		Uterine corpus cancer				
12	68	Squamous cell carcinoma	IIB	4	12.53	7.07
13	36	Squamous cell carcinoma	IIB	3	9.49	4.43
14	47	Squamous cell carcinoma	IIB	7.5	14.57	5.27
15	53	Squamous cell carcinoma	IIB	3.7	10.95	5.53
16	54	Spindle cell carcinoma	IB	0.9	FN	3.86
17	75	Ovarian mucinous cystadenocarcinoma	IA	12	9.31	2.42
18	51	Pelvic inflammatory disease	NA	5	8.13 (FP)	6.02 (FP)
		Recurrent tumor (n = 3)				
19	66	Ovarian serous adenocarcinoma	NA	1.5	3.75	3.63
20	69	Ovarian serous adenocarcinoma	NA	2	FN	FN
21	47	Ovarian serous adenocarcinoma	NA	NA	FN	FN

FN = false-negative; NA = not applicable; FP = false-positive.
Tumor size is longest diameter.

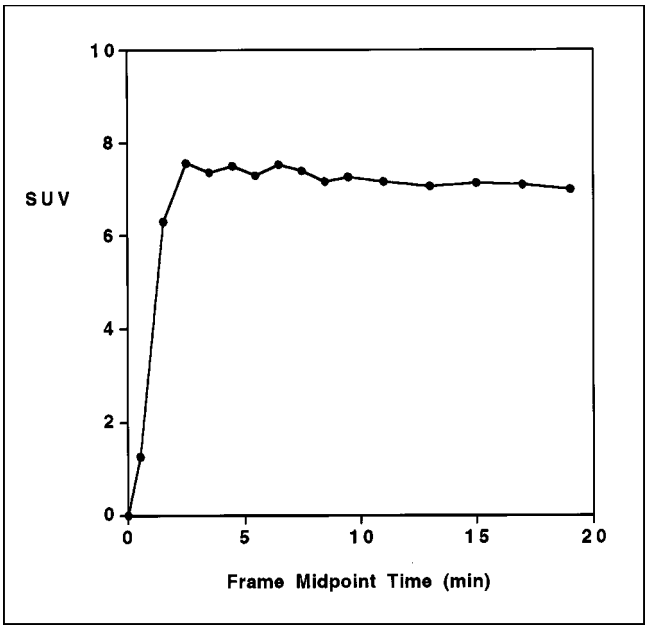

FIGURE 1. Time–activity curve of ^{11}C-choline PET in patient with uterine cervical cancer (patient 12) shows rapid initial uptake in tumor tissue with almost constant level afterward.

choline. For 3 patients suspected of having recurrent ovarian cancer, we performed whole-body ^{11}C-choline PET for the detection of metastatic diseases. Transmission scanning was performed with 5 bed positions for 5 min each, and static emission scanning was performed over the same area for 6 min per bed position, starting 5 min after injection of ^{11}C-choline (600–700 MBq). For the remaining 15 patients, we performed ^{11}C-choline PET scanning covering the pelvis and lower abdominal region. After transmission scanning with 2 bed positions for 8 min each, static emission scanning was performed over the same area for 10 min per bed position, starting 5 min after injection of ^{11}C-choline (500–600 MBq).

Image Analysis

Transaxial, coronal, and sagittal images were reconstructed by a filtered backprojection algorithm with a 128 × 128 matrix. The average reconstructed *x–y* spatial in-plane resolution was about 3.0–4.0 mm in full width at half maximum. For qualitative analysis, any foci of tracer uptake that were increased relative to the background and were not in areas of physiologically increased uptake were considered positive lesions. For quantitative analysis of tracer uptake in tumor, a computerized semiautomated algorithm was used to eliminate interobserver discrepancy. This method helps to define the maximal uptake in a small, square (1.0 × 1.0 cm [3 × 3 pixels]) region of interest (ROI) placed within a large ROI covering the whole tumor and resulted in 100% agreement between 2 observers. In the patients who underwent dynamic ^{11}C-choline PET imaging, the 6th to 13th frames of the dynamic acquisition (6–16 min after injection) were used to define the ROI. As an index of tracer uptake, standardized uptake value (SUV; i.e., tracer activity per injected dose normalized to body weight) was determined for each patient. The mean SUV within an ROI was used to represent tumor uptake of ^{11}C-choline and ^{18}F-FDG. The findings of ^{11}C-choline PET and ^{18}F-FDG PET were compared with the histologic findings at surgery for 19 patients and with >6 mo of clinical observation for 2 patients (patients 19 and 21).

Statistical Analysis

Tumor SUVs of ^{11}C-choline and ^{18}F-FDG were compared using the paired *t* test. A 2-sided *P* value < 0.05 was considered significant.

RESULTS

In 18 patients who underwent PET examinations before surgery, the histology of the primary tumor was uterine corpus cancer ($n = 11$), uterine cervical cancer ($n = 5$), ovarian cancer ($n = 1$), and pelvic inflammatory disease ($n = 1$) (Table 1). In the 11 patients with corpus cancer, surgical FIGO staging was stage IIIA (invasion of serosa) in 2 patients, stage IC (invasion of more than half of the myometrium) in 1 patient, stage IB (invasion of less than half of the myometrium) in 5 patients, stage IA (tumor limited to the endometrium) in 2 patients, and stage 0 (atypical hyperplasia) in 1 patient. For the detection of uterine corpus cancer, both ^{11}C-choline PET and ^{18}F-FDG PET were true-positive in 9 patients. Both tracers were false-negative in 1 patient with atypical hyperplasia of the endometrium (patient 11). In 1 patient with diabetes (patient 10), ^{11}C-choline PET could clearly detect clear cell carcinoma whereas ^{18}F-FDG PET was false-negative, probably because of hyperglycemia (Fig. 2). Serum glucose levels were 188 mg/dL (10.4 mmol/L) and 177 mg/dL (9.8 mmol/L) at the time of ^{11}C-choline PET and ^{18}F-FDG PET,

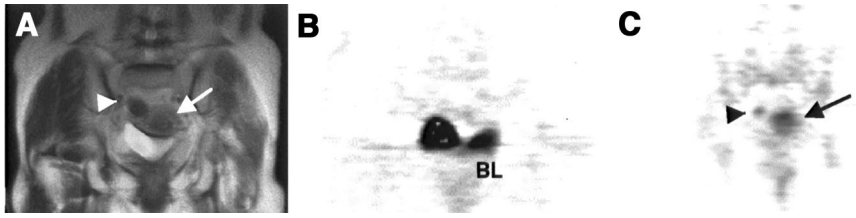

FIGURE 2. Coronal T2-weighted MR image (A) shows enlarged isointense area of endometrium (arrow), indicating presence of tumor. Arrowhead points to intestine. This patient was diabetic. Blood sugar levels were 177 mg/dL (9.8 mmol/L) and 188 mg/dL (10.4 mmol/L) at time of ^{18}F-FDG PET and ^{11}C-choline PET, respectively. In ^{18}F-FDG PET image (B), tumor uptake is negative in presence of hyperglycemia. ^{11}C-Choline PET image (C) demonstrates increased tracer uptake (arrow), corresponding to endometrial tumor. ^{11}C-Choline accumulation in bladder was only minimal, but small hot spot was seen in intestine (arrowhead). Surgical histologic examination revealed clear cell carcinoma (stage IB). BL = bladder activity.

respectively. For nodal staging, both PET studies were true-negative, as proven by surgery, in all 11 of these patients.

^{11}C-Choline PET clearly showed uterine cervical cancer in all 5 patients because of low urinary radioactivity. ^{18}F-FDG PET failed to detect small cervical cancer in 1 patient (stage IB; clinical lesion confined to cervix) (patient 16) in the presence of high bladder activity (Fig. 3). In the other 4 patients with large tumors (stage IIB; parametrial involvement), ^{18}F-FDG PET could show the primary tumors although the tumor visualization was partly hampered by intense bladder activity. For nodal staging, 3 patients had no lymph node metastasis on either PET study, and the lack of metastases was later confirmed by surgery. In the other 2 patients, with enlarged parailiac lymph nodes shown by MRI (patients 14 and 15), ^{18}F-FDG PET clearly detected intense uptake corresponding to the lymphadenopathy. ^{11}C-Choline PET could show the abnormal activity but the visualization was obscured by physiologic bowel uptake (Fig. 4). After transarterial infusion of chemotherapy, lymphadenopathy was not seen on follow-up MR images for 1 patient (patient 15) and surgical histology was negative for metastasis, whereas surgical histology for another patient (patient 14) showed that lymph nodes were still positive for metastasis.

In 1 patient with ovarian mucinous cystadenocarcinoma (patient 17), both ^{11}C-choline PET and ^{18}F-FDG PET showed a large cold area and small hot areas in the primary tumor, corresponding to, respectively, the large cystic lesion and small solid tumors containing adenocarcinoma cells in surgical histology. In 1 patient with pelvic inflammatory disease (infection of *Escherichia coli*) (patient 18), both tracers showed false-positive findings. The SUVs of the lesion were 6.02 for ^{11}C-choline and 8.13 for ^{18}F-FDG. In this case, the pelvic lesion mimicked advanced ovarian cancer in clinical findings as well as in MRI findings before surgery.

Of 3 patients suspected of having recurrence of ovarian cancer, 1 patient showed true-positive results on both ^{11}C-choline PET and ^{18}F-FDG PET for the detection of paraaortic lymph node metastasis in the abdomen, and these results were confirmed by clinical observation (patient 19) (Fig. 5). In the other 2 patients, both PET studies were false-negative. One patient had cystic recurrent disease proven by repeated surgery (patient 20), and 1 patient was considered to have microscopic peritoneal disease on clinical follow-up (patient 21).

Of 21 patients we studied, both ^{11}C-choline PET and ^{18}F-FDG PET findings were true-positive in 15 patients, false-negative in 3 patients, and false-positive in 1 patient for the detection of primary tumor or recurrent tumor. Only ^{11}C-choline PET findings were true-positive in 2 patients. Although ^{11}C-choline PET showed higher sensitivity than ^{18}F-FDG PET for tumor detection (85.0% vs. 75.0%), the mean SUV of ^{11}C-choline was significantly lower, compared with ^{18}F-FDG, in the 15 patients with true-positive results for both tracers (4.61 ± 1.61 vs. 9.14 ± 3.78, $P < 0.0001$). The PET results were not correlated with tumor staging or histologic grade because of the limited number of patients.

DISCUSSION

This study demonstrated the feasibility of ^{11}C-choline PET for imaging gynecologic tumors. For the detection of primary gynecologic tumors in 18 patients, both ^{11}C-choline PET and ^{18}F-FDG PET were true-positive in 14 patients, false-negative in 1 patient, and false-positive in 1 patient. In the other 2 patients, however, only ^{11}C-choline PET could correctly detect the primary tumors. In 1 patient with small uterine cervical cancer, the tumor visualization was hampered by the abundant urinary radioactivity in ^{18}F-FDG PET (Fig. 3). Although bladder irrigation using catheter or adequate hydration may reduce the bladder activity, these methods are complicated and may not completely resolve this problem. On the contrary, urinary ^{11}C-choline activity is negligible or very low; thus, it dose not interfere with PET imaging (*19*). In 1 diabetic patient with uterine corpus cancer, ^{18}F-FDG PET failed to detect the primary tumor, probably because of hyperglycemia (177 mg/dL, 9.8 mmol/L) (Fig. 2). It is well known that tumor ^{18}F-FDG accumulation is impaired in hyperglycemic conditions, presumably by means of direct competition between ^{18}F-FDG and glucose for uptake by cancer cells (*20,21*). With ^{11}C-choline PET, however, the primary uterine cancer was clearly visualized even at the high serum glucose level (188 mg/dL, 10.4 mmol/L), suggesting that ^{11}C-choline can be

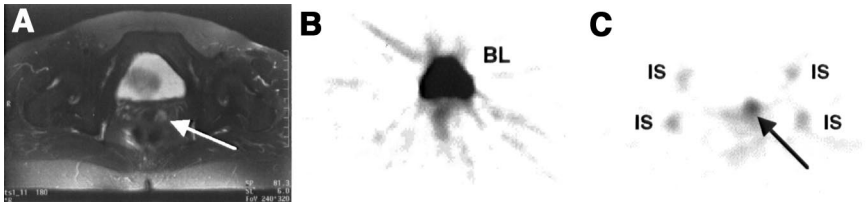

FIGURE 3. Transaxial T2-weighted MR image (A) shows small hyperintense lesion in uterine cervix (arrow). In ^{18}F-FDG PET image (B), tumor visualization is obscured by high bladder activity. ^{11}C-Choline PET image (C) clearly shows intense tumor uptake (arrow), corresponding to cervical cancer. No bladder activity is seen in ^{11}C-choline PET image. Surgical histologic examination revealed spindle cell carcinoma (9×6 mm, stage IB). BL = bladder activity; IS = physiologic uptake of ^{11}C-choline in bilateral ischia.

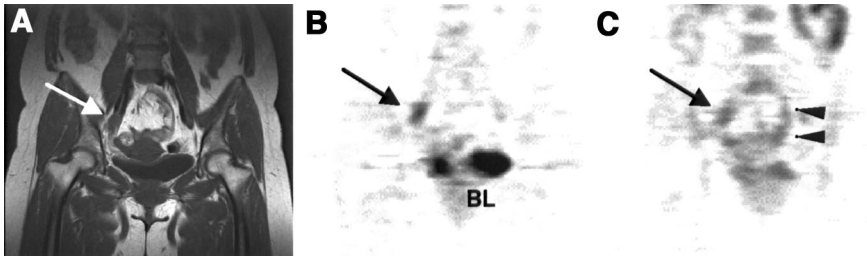

FIGURE 4. Coronal T1-weighted MR image (A) demonstrates right parailiac lymphadenopathy (arrow) in patient with uterine cervical cancer. ^{18}F-FDG PET image (B) clearly shows intense uptake in right parailiac region (arrow), indicating lymph node metastasis. Although ^{11}C-choline PET image (C) detects abnormal activity (arrow), physiologic bowel uptake (arrowheads) mimics parailiac lymph node metastases. Lymphadenopathy was not seen on follow-up MR images after transarterial infusion of chemotherapy. BL = bladder activity.

used for tumor imaging in diabetic patients with hyperglycemia.

For the diagnosis of recurrent diseases in 3 patients, ^{11}C-choline PET and ^{18}F-FDG PET could show a para-aortic lymph node metastasis in 1 patient (Fig. 5) whereas both tracers failed to detect the cystic recurrent tumor and microscopic disseminating disease in the other 2 patients. It has been demonstrated that ^{18}F-FDG PET may miss cystic recurrent tumors or microscopic recurrent diseases in ovarian cancers (*4*,*22*). Similarly, ^{11}C-choline PET may not be able to detect such diseases with a small tumor volume, probably because of the limitations of PET imaging technique.

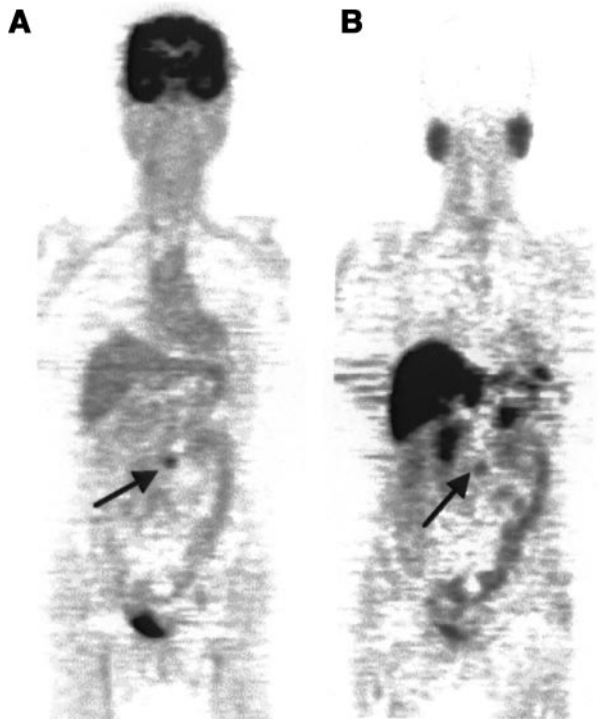

FIGURE 5. Whole-body ^{18}F-FDG PET (A) and ^{11}C-choline PET (B) images show hot spot in para-aortic lymph node metastasis (arrows) in patient with recurrent ovarian cancer. High physiologic uptake of ^{11}C-choline in liver, pancreas, and intestine hampers interpretation of abdomen and pelvis.

Compared with ^{18}F-FDG PET, ^{11}C-choline PET has the advantage of providing a clear image at an earlier period (*11*,*13*,*23*). In ^{18}F-FDG PET, patients have to wait for 60 min or longer after tracer injection for tumor activity to reach the peak count (*24*). With ^{11}C-choline, however, blood clearance is rapid and tumor activity reaches a maximum at 3–5 min after injection. The initial intense uptake remains at a nearly constant level afterward, thus enabling the high activity ratio to remain for more than 30 min, compared with background.

The mechanism for cellular uptake of choline has not been completely clarified. In mammalian cells, 2 transport mechanisms have been identified: energy-dependent choline-specific transport and simple diffusion (*25*,*26*). In our case, both ^{11}C-choline and ^{18}F-FDG strongly accumulated in pelvic inflammatory disease, although ^{18}F-FDG uptake was more intense. In other studies, we have found intense ^{11}C-choline uptake in inflammatory lesions such as radiation pneumonitis and sarcoidosis. It appears that ^{11}C-choline uptake into inflammatory lesions might be associated with the influence of simple diffusion in the reactive tissues.

Our study demonstrated that the tumor SUV was significantly lower for ^{11}C-choline than for ^{18}F-FDG. This observation is consistent with previous results for patients with lung cancers (*27*) and esophageal cancers (*23*,*28*). Because ^{11}C-choline is a metabolic tracer, one may assume that ^{11}C-choline uptake is related to the proliferation of tumors. In all animal cells, choline is used as a precursor for the biosynthesis of phospholipids, including phosphatidylcholine, which are essential components of all membranes and modulate signaling processes and the apoptosis pathway within cells (*29*). The relationship between intracellular choline metabolism and cell proliferation is currently under investigation.

The physiologic body distribution of ^{11}C-choline is different from that of ^{18}F-FDG. High ^{11}C-choline uptake is normally observed in the liver and kidney (cortex), where choline is converted into betaine, and in the pancreas and duodenum because of the secretion of phospholipid-rich pancreatic juice (*7*,*11*). Furthermore, ^{11}C-choline uptake is usually present to various degrees in the small intestine and

colon (Fig. 5). This physiologic ^{11}C-choline uptake may make it difficult to adequately interpret PET images of the pelvis and abdomen. In contrast, physiologic background levels of ^{18}F-FDG are lower in the abdomen and pelvis, except for the urinary tract. In our study, the interpretation of parailiac lymph node metastases was hampered by bowel ^{11}C-choline uptake, whereas ^{18}F-FDG clearly showed the parailiac lesion (Fig. 4). In the study of esophageal cancer, ^{18}F-FDG PET showed higher sensitivity than ^{11}C-choline PET for the detection of metastatic lesions in the abdomen (*23*). Thus, ^{11}C-choline may be inferior to ^{18}F-FDG for the staging of tumors in the abdomen and pelvis, although further studies are needed to confirm this possibility.

CONCLUSION

Our preliminary study indicated that the use of ^{11}C-choline PET may be feasible for the imaging of gynecologic tumors. ^{11}C-Choline PET can clearly detect primary tumors because of low urinary activity; however, variable physiologic accumulation of ^{11}C-choline in the intestine may be a problem.

REFERENCES

1. Eubank WB, Mankoff DA, Takasugi J, et al. 18fluorodeoxyglucose positron emission tomography to detect mediastinal or internal mammary metastases in breast cancer. *J Clin Oncol.* 2001;19:3516–3523.
2. Eschmann SM, Friedel G, Paulsen F, et al. FDG PET for staging of advanced non-small cell lung cancer prior to neoadjuvant radio-chemotherapy. *Eur J Nucl Med Mol Imaging.* 2002;29:804–808.
3. Kalff V, Hicks RJ, Ware RE, Hogg A, Binns D, McKenzie AF. The clinical impact of (18)F-FDG PET in patients with suspected or confirmed recurrence of colorectal cancer: a prospective study. *J Nucl Med.* 2002;43:492–499.
4. Torizuka T, Nobezawa S, Kanno T, et al. Ovarian cancer recurrence: role of whole-body positron emission tomography using 2-[fluorine-18]-fluoro-2-deoxy-D-glucose. *Eur J Nucl Med Mol Imaging.* 2002;29:797–803.
5. Sugawara Y, Eisbruch A, Kosuda S, Recker BE, Kison PV, Wahl RL. Evaluation of FDG PET in patients with cervical cancer. *J Nucl Med.* 1999;40:1125–1131.
6. Williams AD, Cousins C, Soutter WP, et al. Detection of pelvic lymph node metastases in gynecologic malignancy: a comparison of CT, MR imaging, and positron emission tomography. *AJR.* 2001;177:343–348.
7. Roivainen A, Forsback S, Gronroos T, et al. Blood metabolism of [methyl-^{11}C]choline; implications for in vivo imaging with positron emission tomography. *Eur J Nucl Med.* 2000;27:25–32.
8. Zeisel SH. Dietary choline: biochemistry, physiology, and pharmacology. *Annu Rev Nutr.* 1981;1:95–121.
9. Miller BL, Chang L, Booth R, et al. In vivo 1H MRS choline: correlation with in vitro chemistry/histology. *Life Sci.* 1996;58:1929–1935.
10. Tedeschi G, Lundbom N, Raman R, et al. Increased choline signal coinciding with malignant degeneration of cerebral gliomas: a serial proton magnetic resonance spectroscopy imaging study. *J Neurosurg.* 1997;87:516–524.
11. Hara T, Kosaka N, Shinoura N, Kondo T. PET imaging of brain tumor with [methyl-^{11}C]choline. *J Nucl Med.* 1997;38:842–847.
12. Shinoura N, Nishijima M, Hara T, et al. Brain tumors: detection with C-11 choline PET. *Radiology.* 1997;202:497–503.
13. Kotzerke J, Prang J, Neumaier B, et al. Experience with carbon-11 choline positron emission tomography in prostate carcinoma. *Eur J Nucl Med.* 2000;27:1415–1419.
14. Hara T, Kosaka N, Kishi H. PET imaging of prostate cancer using carbon-11-choline. *J Nucl Med.* 1998;39:990–995.
15. Shepherd JH. Revised FIGO staging for gynaecological cancer [published correction appears in *Br J Obstet Gynaecol.* 1992;99:440]. *Br J Obstet Gynaecol.* 1989;96:889–892.
16. Lindholm P, Minn H, Leskinen-Kallio S, Bergman J, Ruotsalainen U, Joensuu H. Influence of the blood glucose concentration on FDG uptake in cancer: a PET study. *J Nucl Med.* 1993;34:1–6.
17. Torizuka T, Nobezawa S, Momiki S, et al. Short dynamic FDG-PET imaging protocol for patients with lung cancer. *Eur J Nucl Med.* 2000;27:1538–1542.
18. Hamacher K, Coenen HH, Stocklin G. Efficient stereospecific synthesis of no-carrier-added 2-[^{18}F]-fluoro-2-deoxy-D-glucose using aminopolyether supported nucleophilic substitution. *J Nucl Med.* 1986;27:235–238.
19. de Jong IJ, Pruim J, Elsinga PH, Jongen MM, Mensink HJ, Vaalburg W. Visualisation of bladder cancer using (11)C-choline PET: first clinical experience. *Eur J Nucl Med.* 2002;29:1283–1288.
20. Wahl RL, Henry CA, Ethier SP. Serum glucose: effects on tumor and normal tissue accumulation of 2-[F-18]-fluoro-2-deoxy-D-glucose in rodents with mammary carcinoma. *Radiology.* 1992;183:643–647.
21. Torizuka T, Clavo AC, Wahl RL. Effect of hyperglycemia on in vitro tumor uptake of tritiated FDG, thymidine, L-methionine and L-leucine. *J Nucl Med.* 1997;38:382–386.
22. Rose PG, Faulhaber P, Miraldi F, Abdul-Karim FW. Positron emission tomography for evaluating a complete clinical response in patients with ovarian or peritoneal carcinoma: correlation with second-look laparotomy. *Gynecol Oncol.* 2001;82:17–21.
23. Jager PL, Que TH, Vaalburg W, Pruim J, Elsinga P, Plukker JT. Carbon-11 choline or FDG-PET for staging of oesophageal cancer? *Eur J Nucl Med.* 2001;28:1845–1849.
24. Kubota K, Itoh M, Ozaki K, et al. Advantage of delayed whole-body FDG-PET imaging for tumour detection. *Eur J Nucl Med.* 2001;28:696–703.
25. Katz-Brull R, Degani H. Kinetics of choline transport and phosphorylation in human breast cancer cells: NMR application of the zero *trans* method. *Anticancer Res.* 1996;16:1375–1380.
26. Ishidate K. Choline transport and choline kinase. In: Vance DE, ed. *Phosphatidylcholine Metabolism.* Boca Raton, FL: CRC Press; 1989:9–32.
27. Pieterman RM, Que TH, Elsinga PH, et al. Comparison of (11)C-choline and (18)F-FDG PET in primary diagnosis and staging of patients with thoracic cancer. *J Nucl Med.* 2002;43:167–172.
28. Kobori O, Kirihara Y, Kosaka N, Hara T. Positron emission tomography of esophageal carcinoma using (11)C-choline and (18)F-fluorodeoxyglucose: a novel method of preoperative lymph node staging. *Cancer.* 1999;86:1638–1648.
29. Zeisel SH. Choline phospholipids: signal transduction and carcinogenesis. *FASEB J.* 1993;7:551–557.